ORIGINAL PAPER

High-spin binuclear cyclopentadienyliron chlorides: a density functional theory study

Congzhi Wang · Xiuhui Zhang · Yang Bai · Fengxin Gao · Qianshu Li

Abstract Theoretical studies on the cyclopentadienyliron chlorides $Cp_2Fe_2Cl_n$ ($n=6-1$) with iron in the formal oxidation states from +1 to +4 indicate that all the high-spin species are predicted to be the lowest energy structures and they are paramagnetic complexes with magnetic moments between $2.8\mu_B$ and $5.9\mu_B$. The mixed oxidation state derivatives with odd number of chloride atoms have larger magnetic moments than other species. In addition to Cp_2Fe_2Cl, which has the largest magnetic moment, these high-spin species have terminal Cp rings and bridging Cl atoms up to a maximum of two bridges. The $Cp_2Fe_2Cl_4$, $Cp_2Fe_2Cl_3$ and $Cp_2Fe_2Cl_2$ derivatives are predicted to be thermodynamically stable molecules with respect to exothermic reactions for the loss of one Cl atom from $Cp_2Fe_2Cl_n$. Moreover, the lowest energy $Cp_2Fe_2Cl_n$ ($n=3$, 4) derivatives can be derived by the oxidative addition reactions of $Cp_2Fe_2Cl_{n-2} + Cl_2 \rightarrow Cp_2Fe_2Cl_n$.

C. Wang · X. Zhang (✉) · Y. Bai · F. Gao
Key Laboratory of Cluster Science, Ministry of Education of China, School of Chemistry, Beijing Institute of Technology, Beijing 100081, People's Republic of China
e-mail: zhangxiuhui@bit.edu.cn

C. Wang
Nuclear Energy Nano-Chemistry Group, Key Laboratory of Nuclear Analytical Techniques and Key Laboratory For Biomedical Effects of Nanomaterials and Nanosafety, Institute of High Energy Physics, Chinese Academy of Sciences, Beijing 100049, People's Republic of China

Q. Li (✉)
Institute of Chemical Physics, Beijing Institute of Technology, Beijing 100081, People's Republic of China
e-mail: qsli@bit.edu.cn

Q. Li
MOE Key Laboratory of Theoretical Chemistry of Environment, Center for Computational Quantum Chemistry, South China Normal University, Guangzhou 510006, People's Republic of China

Introduction

Since the first sandwich-like compound ferrocene Cp_2Fe ($Cp = \eta^5\text{-}C_5H_5$), was discovered in 1951 [1], the chemistry of cyclopentadienyl metal complexes has developed rapidly. In the past decades, a series of dicyclopentadienyl transition metal sandwich-like complexes have been reported, such as Cp_2V, Cp_2Cr, Cp_2Co, and Cp_2Ni *etc.* [2–5]. It is well known that most of these isolable organometallic compounds are low-spin species and they are diamagnetic, which satisfy the closed-shell requirement. Whereas, some high-spin organometallic complexes, which usually contain the $3d^n$ ($n=2–8$) transition metal atoms, have also been reported [6]. Moreover, these high-spin complexes have some special physical properties, such as conductivity, magnetism, and optical effects [7–9]. Among these complexes, there is a growing interest in the chemistry of high-spin organometallic iron compounds because the iron complexes play an important role in magnetic materials [10].

For the organometallic iron complexes, some high-spin paramagnetic complexes with iron in different formal oxidation states have been found. Among them, the common paramagnetic iron complexes are the ferrocenium cations with iron in the +3 oxidation states, such as $[Fe^{III}(C_5H_4CH_2C_5H_4)_2Ru^{II}]^+$ and $[Fe^{III}Cp(C_5H_4CH_2C_5H_4)CpRu^{IV}I]^{2+}$ which have one unpaired electron [11–13]. However, some high-spin organometallic iron complexes with iron in +1 and +4 formal oxidation states have also been reported. For iron(I) complexes, Bursten *et al.* [14] reported the preparation of an 18-electron species

Cp*$_2$Fe$_2$(μ-CO)$_3$ (Cp* = C$_5$Me$_5$), which has a triplet ground state and exhibits paramagnetic. Its highest occupied molecular orbital (HOMO) is a two-fold degenerate antibonding orbital with π symmetry, which is similar to the electronic structure of O$_2$. For iron(IV) complexes, the dication [Cp*$_2$Fe]$^{2+}$, which can be stable for at least 4 h in solution at −30 °C, is paramagnetic with two unpaired electrons [15].

Furthermore, many high-spin organometallic iron(II) complexes have also already been found. For instance, Girolam et al. [16] isolated a series of iron(II) complexes FeR$_2$(dippe) (R = CH$_2$SiMe$_3$, CH$_2$CMe$_3$, CH$_2$CMe$_2$Ph, CH$_2$Ph, CH$_2$C$_6$H$_4$Me; dippe = 1,2-bis(diisopropyl phosphino) ethane) and found that they are high-spin (four unpaired electrons) species and possess magnetic moments characteristic (μ= 4.9μ$_B$). Lapinte et al. [17] isolated the first paramagnetic six-coordinated 18-electron iron(II) organometallic complex, [Cp*Fe(η^2-dppe)(σ-O = CMe$_2$]$^+$CF$_3$SO$_3^-$ (dppe = Ph$_2$PCH$_2$CH$_2$PPh$_2$) with two unpaired electrons. They also reported a half-sandwich iron(II) 16-electron complex [Cp*Fe(dppe)][PF$_6$] and confirmed that it exhibits an effective magnetic moment μ_{eff} = 3.3μ$_B$ in tetrahydrofuran solution corresponding to two unpaired electrons [18]. In addition to these high-spin mononuclear iron(II) complexes, some binuclear iron(II) halides with bulky substituted cyclopentadienyl have also been reported. In 1996, Sitzmann et al. [19] prepared the paramagnetic complex [(C$_5$HR$_4$)FeBr]$_2$ (R = CHMe$_2$), containing d^6 Fe(II) with four unpaired electrons. Recently, Walter et al. [20] synthesized three halide-bridged complexes [Cp′FeX]$_2$ (Cp′ = 1,2,4-$_t$Bu$_3$C$_5$H$_2$; X = Cl, Br, I), which contain high-spin iron(II) centers with four unpaired electrons. These discoveries indicate that the introduction of extremely bulky substituted cyclopentadienyl ligands into metallocene of the iron metals may be required to generate maximum spin cyclopentadienyl complexes [13].

Since the magnetic properties of the cyclopentadienyliron complexes are influenced by substituents on the cyclopentadienyl ligands, a question of interest is whether the coordination numbers affect their magnetic properties. In the present paper, a series of sandwich-like complexes Cp$_2$Fe$_2$Cl$_n$ (n=6−1) with one to six chlorine atoms as well as the iron atoms in the formal oxidation states between +4 and +1 selected as model complexes have been investigated by density functional theory (DFT) in order to provide information on the equilibrium geometries and the relative stabilities as well as magnetic behavior of these complexes. The theoretical studies reported in this paper were performed using the unsubstituted η^5-C$_5$H$_5$ ligand in order to simplify the optimizations in this exploratory research.

Theoretical methods

Electron correlation effects were included by employing density functional theory (DFT) methods, which have evolved as a practical and effective computational tool, especially for organometallic compounds [21–29]. Three DFT methods were used in this study. The first functional is the B3LYP model, which is a hybrid HF-DFT method using Becke's three-parameter exchange functional (B3) with the Lee, Yang, and Parr (LYP) correlation functional [30, 31]. The second approach is the new generation functional MPW1PW91, which is a combination of the modified Perdew-Wang exchange functional with Perdew-Wang's 91 gradient-correlation functional [32]. The third one is BP86 method, which combines Becke's 1988 exchange functional (B) with Perdew's 1986 correlation functional method (P86) [33, 34]. The B3LYP and MPW1PW91 methods have been found to be suitable for predicting the molecular structures of metallocenes, while the BP86 method usually provides better vibrational frequencies [35, 36]. In the present study, the B3LYP and MPW1PW91 methods agree with each other well in predicting the structural characteristics of Cp$_2$Fe$_2$Cl$_n$. Thus, the B3LYP and MPW1PW91 results (geometries and energies) are discussed in the text, and the BP86 results (geometries, energies, and vibrational frequencies) are given in the Supporting information.

All computations were performed using double-ζ plus polarization (DZP) basis sets. For carbon, the DZP basis set used here adds one set of pure spherical harmonic d functions (with orbital exponent $\alpha_d(C)$ = 0.75) to the Huzinaga-Dunning standard contracted DZ sets and is designated (9s5p1d/4s2p1d) [37, 38]. For chlorine, the DZP basis set used here adds one set of pure spherical harmonic d functions (with orbital exponent $\alpha_d(Cl)$ = 0.75) to the Huzinaga-Dunning-Hay standard contracted DZ sets and is designated (12s8p1d/6s4p1d) [37, 38]. For hydrogen, a set of p polarization functions ($\alpha_p(H)$ = 0.75) is added to the Huzinaga-Dunning DZ sets. For iron, the loosely contracted DZP basis set (14s11p6d/10s8p3d) is the Wachters primitive set [39] augmented by two sets of p functions and a set of d functions following Hood, Pitzer, and Schaefer [40].

The geometries of all of the structures were fully optimized using both the DZP B3LYP, DZP MPW1PW91 and DZP BP86 methods. The harmonic vibrational frequencies were determined at the same levels by evaluating analytically the second derivatives of the energy with respect to the nuclear coordinates. The corresponding infrared intensities were evaluated analytically as well. All of the computations were carried out with the Gaussian 03 program [41]. The fine grid (75, 302) was the default for evaluating integrals numerically [42]. The finer grid (120, 974) was used for

more precise resolution of the small imaginary vibrational frequencies. The tight (10^{-8} hartree) designation was the default for the self-consistent field (SCF) convergence.

Since there is no wave function *per se* in the DFT method, the evaluation of the expectation value of S^2 is problematic. The most realistic and practical method is to evaluate $\langle S^2 \rangle$ using the single determinant constructed from the appropriate DFT orbitals. When DFT methods for open-shell systems perform poorly, one very often observes serious spin contamination in the sense defined here.

The structures for $Cp_2Fe_2Cl_n$ ($n=6-1$) are labeled by the number of Cl atoms, order of relative energies, and spin state (sextets, quartets, triplets, doublets, and singlets designated as **SE, Q, T, D** and **S** respectively). For example, the quartet energetically lowest-lying structure of $Cp_2Fe_2Cl_5$ is called **5Cl-1Q**. The upper and lower bond distances in the Figs. were determined by the B3LYP and MPW1PW91 methods, respectively.

Results

There are two general types of structures for $Cp_2Fe_2Cl_n$ derivatives ($n=6-1$). Firstly, the coaxial structures, in which each Cp ring is only bonded to a single metal atom so that the C_5 axes of the Cp rings are approximately collinear with the Fe–Fe bond. Secondly, the perpendicular structures, in which each Cp ring bridges both metal atoms so that the Fe–Fe axis is approximately perpendicular to the C_5 axes of the Cp rings.

$Cp_2Fe_2Cl_6$

For $Cp_2Fe_2Cl_6$ with the iron atoms in the formal oxidation state of +4, there are one triplet and two singlet coaxial structures (Fig. 1). They all have real vibrational frequencies, indicating that they are genuine minima on the energy surface. The global minimum predicted for $Cp_2Fe_2Cl_6$ is a triplet C_1 structure **6Cl-1T** with one three-electron donor bridging μ-Cl ligand and five terminal Cl ligands. The spin contamination is not serious, *i.e.*, $\langle S^2 \rangle = 2.23$ (B3LYP) or $\langle S^2 \rangle = 2.30$
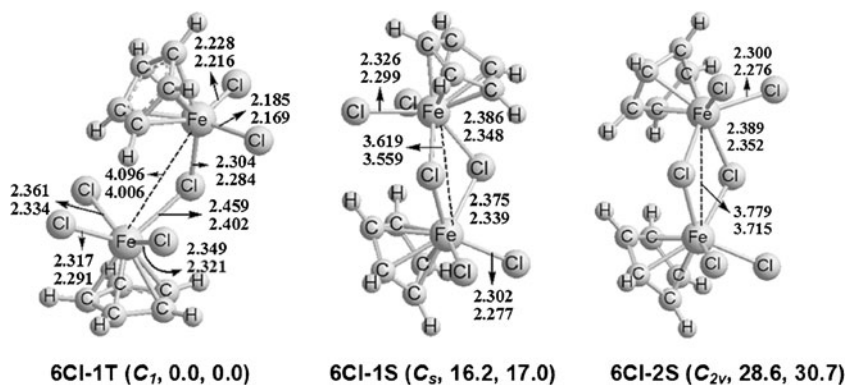
(MPW1PW91) versus an ideal $S(S+1) = 2.00$ for a triplet. The Fe-Cl distances to the bridging Cl ligand are 2.304 and 2.459 Å (B3LYP) or 2.284 and 2.402 Å (MPW1PW91). The Fe-Fe distance in **6Cl-1T** is predicted to be 4.096 Å (B3LYP) or 4.006 (MPW1PW91), indicating the lack of a direct iron-iron bond, which is required to give each iron atom the 17-electron configuration for a binuclear triplet. Thus, each iron atom in **6Cl-1T** has one unpaired electron and the calculated magnetic moment of **6Cl-1T** is $2.8\mu_B$.

Two singlet $Cp_2Fe_2Cl_6$ structures were found, namely, the *trans* (**6Cl-1S**) and *cis* (**6Cl-2S**) doubly bridged structures (Fig. 1). Structure **6Cl-1S** is a C_s structure which lies 16.2 kcal mol^{-1} (B3LYP) or 17.0 kcal mol^{-1} (MPW1PW91) above the global minimum **6Cl-1T**, while **6Cl-2S** is a C_{2v} structure and lies at the relatively high energy of 28.6 kcal mol^{-1} (B3LYP) or 30.7 kcal mol^{-1} (MPW1PW91) above **6Cl-1T**. The Fe-Fe distances in **6Cl-1S** and **6Cl-2S** are very long, namely, 3.619 and 3.779 Å by B3LYP or 3.559 and 3.715 Å by MPW1PW91, respectively, indicating the absence of direct iron-iron bonds. Thus, in **6Cl-1S** and **6Cl-2S**, each iron atom has an 18-electron configuration, corresponding to a binuclear singlet.
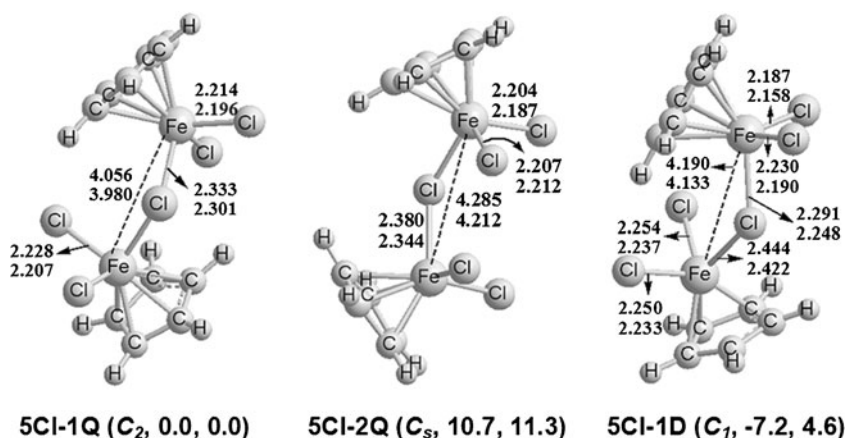
$Cp_2Fe_2Cl_5$

For $Cp_2Fe_2Cl_5$ with iron atoms in an average formal oxidation state of +3.5, two quartet structures **5Cl-1Q** and **5Cl-2Q** and one doublet structure **5Cl-1D** were found (Fig. 2). All of these structures are predicted to be coaxial structures, which have one three-electron donor bridging and four terminal Cl ligands. The quartet C_2 *trans* structure **5Cl-1Q** is the global minimum with no imaginary vibrational frequencies and little spin contamination with $\langle S^2 \rangle = 3.99$ by B3LYP or 4.05 by MPW1PW91, which is close to the ideal value $S(S+1) = 3.75$. The Fe-Cl distances to the bridging Cl ligand in **5Cl-1Q** are 2.333 Å (B3LYP) or 2.301 (MPW1PW91), and the Fe-Cl distances to the termial Cl ligand are 2.214 and 2.228 Å (B3LYP) or 2.196 and 2.207 Å (MPW1PW91). The Fe-Fe distance in **5Cl-1Q** is predicted to be quite long at 4.056 Å (B3LYP) or 3.980 Å

Fig. 1 Three optimized structures for $Cp_2Fe_2Cl_6$ indicating the relative energies (ΔE, in kcal mol^{-1}) by the B3LYP and MPW1PW91 methods, respectively. The distances are given in Å. The upper distances were obtained by the B3LYP method, while the lower distances were obtained by the MPW1PW91 method. The subsequent figures have the same arrangement

6Cl-1T (C_1, 0.0, 0.0)   6Cl-1S (C_s, 16.2, 17.0)   6Cl-2S (C_{2v}, 28.6, 30.7)

5Cl-1Q (C_2, 0.0, 0.0)   **5Cl-2Q (C_s, 10.7, 11.3)**   **5Cl-1D (C_1, -7.2, 4.6)**

(MPW1PW91), suggesting the absence of a formal iron-iron bond in **5Cl-1Q**. This gives one iron atom in **5Cl-1Q** a 16-electron configuration but the other iron atom a 17-electron configuration, which is consistent with the quartet spin multiplicity. Thus, there are three unpaired electrons in **5Cl-1Q** and the calculated magnetic moment of **5Cl-1Q** is $3.9\mu_B$.

The other quartet $Cp_2Fe_2Cl_5$ structure **5Cl-2Q** is a *cis* structure with C_s symmetry (Fig. 2). Structure **5Cl-2Q** has a small imaginary frequency by B3LYP ($18i$ cm^{-1}) and MPW1PW91 ($22i$ cm^{-1}), and lies 10.7 kcal mol^{-1} (B3LYP) or 11.3 kcal mol^{-1} (MPW1PW91) above the global minimum **5Cl-1Q**. The spin contamination in **5Cl-2Q** is small with $\langle S^2 \rangle$ = 3.91 (B3LYP) or $\langle S^2 \rangle$= 3.93 (MPW1PW91). The Fe-Fe distance in **5Cl-2Q** is long at 4.285 Å (B3LYP) or 4.212 Å (MPW1PW91), suggesting no significant iron-iron interaction. This leads to a 16-electron configuration for one iron atom and a 17-electron configuration for the other iron atom for a binuclear quartet with three unpaired electrons.
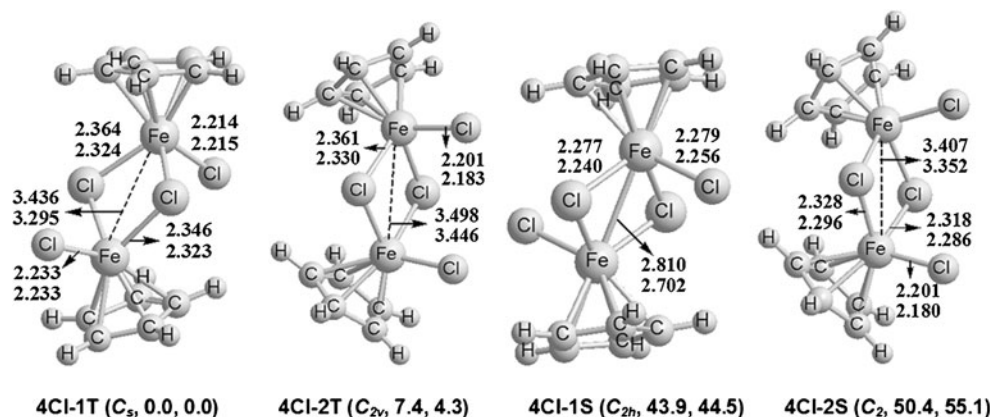
The doublet structure **5Cl-1D** (Fig. 2) is a C_1 *trans* structure with all real vibrational frequencies. The B3LYP method predicts structure **5Cl-1D** to lie 7.2 kcal mol^{-1} below **5Cl-1Q**, while the MPW1PW91 method predicts structure **5Cl-1D** to lie 4.6 kcal mol^{-1} above **5Cl-1Q**. Structure **5Cl-1D** is found to be problematic, having serious spin

contamination with the spin expectation value $\langle S^2 \rangle$ = 2.07 (B3LYP) or 1.84 (MPW1PW91), which is much higher than the ideal 0.75. This may result in relative lower energy than that of the real state. In **5Cl-1D**, the Fe-Cl distances to the bridging Cl ligand are 2.291 and 2.444 Å (B3LYP) or 2.248 and 2.422 Å (MPW1PW91). The Fe-Fe distance for **5Cl-1D** is very long, namely 4.190 Å by B3LYP or 4.133 Å by MPW1PW91, indicating the absence of a chemical bond between the two iron atoms.

$Cp_2Fe_2Cl_4$

There are four possible singlet and triplet structures of $Cp_2Fe_2Cl_4$ with iron in the formal +2 oxidation state, namely, the *trans* (**4Cl-1T**, **4Cl-1S**) and *cis* (**4Cl-2T**, **4Cl-2S**) doubly bridged structures (Fig. 3). The two triplet structures **4Cl-1T** and **4Cl-2T** are predicted to be genuine minima with all real vibrational frequencies. Structure **4Cl-1T** is predicted to be global minimum with C_s symmetry, while **4Cl-2T** is a C_{2v} structure, which lies 7.4 kcal mol^{-1} (B3LYP) or 4.3 kcal mol^{-1} (MPW1PW91) above **4Cl-1T**. There is very little spin contamination for **4Cl-1T** and **4Cl-2T**, i.e., $\langle S^2 \rangle$ = 2.09 (B3LYP) or $\langle S^2 \rangle$ = 2.18 (MPW1PW91), which is close to the ideal value S(S +1) = 2.00. The Fe-Fe distance in **4Cl-1T** and **4Cl-2T** fall in the range 3.295 to 3.498 Å,

4Cl-1T (C_s, 0.0, 0.0)   **4Cl-2T (C_{2v}, 7.4, 4.3)**   **4Cl-1S (C_{2h}, 43.9, 44.5)**   **4Cl-2S (C_2, 50.4, 55.1)**

respectively, suggesting no significant iron-iron interaction. This gives each iron atom in **4Cl-1T** and **4Cl-2T** a 17-electron configuration corresponding to a binuclear triplet with two unpaired electrons. Thus, the calculated magnetic moment of **4Cl-1T** is $2.8\mu_B$.

The singlet C_{2h} structure **4Cl-1S** (Fig. 3) has all real vibrational frequencies by B3LYP and MPW1PW91. Structure **4Cl-1S** lies 43.9 kcal mol^{-1} (B3LYP) or 44.5 kcal mol^{-1} (MPW1PW91) above the global minimum **4Cl-1T**. The Fe-Cl distances to the bridging and terminal Cl ligands are 2.277 and 2.279 Å (B3LYP) or 2.240 and 2.256 Å (MPW1PW91), respectively. The Fe-Fe distance in **4Cl-1S** is 2.810 Å (B3LYP) or 2.702 Å (MPW1PW91), which can correspond to a formal Fe-Fe single bond. However, this presumed Fe-Fe single bond is ~0.3 Å longer than the experimental Fe–Fe single bond distance (2.523 Å) in a binuclear iron carbonyl derivative [43]. The formal Fe–Fe single bond in **4Cl-1S** gives each iron atom the favored 18-electron configuration.

The other singlet $Cp_2Fe_2Cl_4$ structure **4Cl-2S** (Fig. 3) is a C_2 structure with all real vibrational frequencies, which lies 50.4 kcal mol^{-1} (B3LYP) or 55.1 kcal mol^{-1} (MPW1PW91) above **4Cl-1T**. The Fe-Cl distances to the bridging Cl ligands are 2.318 and 2.328 Å (B3LYP) or 2.286 and 2.296 Å (MPW1PW91), while those to the termial Cl ligands are 2.201 Å (B3LYP) or 2.180 Å (MPW1PW91). The Fe-Fe distances in **4Cl-2S** is long at 3.407 Å (B3LYP) or 3.352 Å (MPW1PW91) indicating the absence of a direct Fe-Fe bond.

$Cp_2Fe_2Cl_3$

For $Cp_2Fe_2Cl_3$, which is formally a mixed oxidation state derivative with one Fe(III) atom and one Fe(II) atom, there are seven energetically low-lying structures (Figs. 4 and 5). The $Cp_2Fe_2Cl_3$ global minimum **3Cl-1Q** (Fig. 4) is predicted to be a quartet C_1 structure with all real harmonic frequencies. It has one bridging Cl ligands and the calculated magnetic moment is $3.9\mu_B$. Structure **3Cl-1Q** has some spin contamination, i.e., $\langle S^2 \rangle = 4.82$ (B3LYP) or $\langle S^2 \rangle = 4.84$ (MPW1PW91). In **3Cl-1Q**, the Fe-Cl distances to the
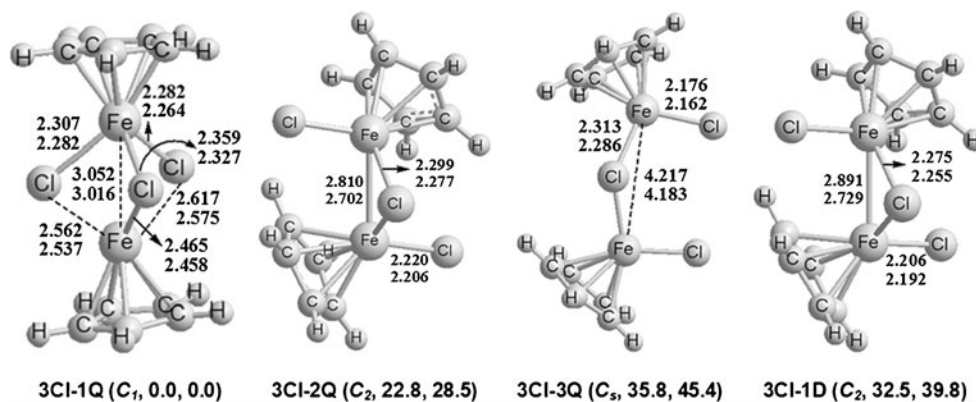
bridging Cl ligand are 2.359 and 2.465 Å (B3LYP) or 2.327 and 2.458 Å (MPW1PW91). The other two Cl ligands can be considered to be semibridging ligands with two short Fe-Cl distances of ~2.3 Å and two relatively long Fe-Cl distances of ~2.6 Å. The Fe-Fe distance is 3.052 Å (B3LYP) or 3.016 Å (MPW1PW91), suggests that there is no direct iron-iron interaction for this structure.

Structure **3Cl-2Q** is a C_2 *trans* structure with one bridging and two terminal Cl ligands lying 22.8 kcal mol^{-1} (B3LYP) or 28.5 kcal mol^{-1} (MPW1PW91) above **3Cl-1Q**. There is relatively little spin contamination for **3Cl-2Q**, i.e., $\langle S^2 \rangle = 4.08$ (B3LYP) or $\langle S^2 \rangle = 4.14$ (MPW1PW91). The Fe-Cl distances to the bridging Cl ligand are 2.299 Å (B3LYP) or 2.277 Å (MPW1PW91), and these distances to the terminal Cl ligands are 2.220 Å (B3LYP) or 2.206 Å (MPW1PW91). The Fe-Fe distance in **3Cl-2Q** is 2.810 Å (B3LYP) or 2.702 Å (MPW1PW91), indicating the iron-iron formal single bond required to give one iron atom a 16-electron configuration and the other iron atom a 17-electron configuration for a binuclear quartet with three unpaired electrons.

The last quartet $Cp_2Fe_2Cl_3$ structure **3Cl-3Q** (Fig. 4) has one bridging and two terminal Cl ligands with C_s symmetry and it lies above **3Cl-1Q** by 35.8 (B3LYP) or 45.4 kcal mol^{-1} (MPW1PW91). Structure **3Cl-3Q** has a small imaginary frequency ($21i$ cm^{-1} or $49i$ cm^{-1} by B3LYP or MPW1PW91) and samll spin contamination $\langle S^2 \rangle = 4.00$ (B3LYP) or $\langle S^2 \rangle = 4.05$ (MPW1PW91). The Fe-Cl distances to the bridging Cl ligand are 2.313 Å (B3LYP) or 2.286 Å (MPW1PW91), and those to the terminal Cl ligands are 2.176 Å (B3LYP) or 2.162 Å (MPW1PW91). The Fe-Fe distance in **3Cl-3Q** is 4.217 Å (B3LYP) or 4.183 Å (MPW1PW91), indicating no direct chemical interaction between the two iron atoms.

The only doublet $Cp_2Fe_2Cl_3$ structure **3Cl-1D** is a C_2 *trans* structure with one bridging and two terminal Cl ligands (Fig. 4). Structure **3Cl-1D** has all real vibrational frequencies by B3LYP, while it has an imaginary frequency by MPW1PW91 ($102i$ cm^{-1}), lying 32.5 kcal mol^{-1} (B3LYP) or 39.8 kcal mol^{-1} (MPW1PW91) above **3Cl-1Q**. It has serious spin contamination with $\langle S^2 \rangle = 1.72$ (B3LYP) or

Fig. 4 Four optimized structures for the quartet and doublet $Cp_2Fe_2Cl_3$ indicating the relative energies (ΔE, in kcal mol^{-1}) by the B3LYP and MPW1PW91 methods, respectively

3Cl-1Q (C_1, 0.0, 0.0)   3Cl-2Q (C_2, 22.8, 28.5)   3Cl-3Q (C_s, 35.8, 45.4)   3Cl-1D (C_2, 32.5, 39.8)

Fig. 5 Three optimized structures for the sextet $Cp_2Fe_2Cl_3$ indicating the relative energies (ΔE, in kcal mol^{-1}) by the B3LYP and MPW1PW91 methods, respectively
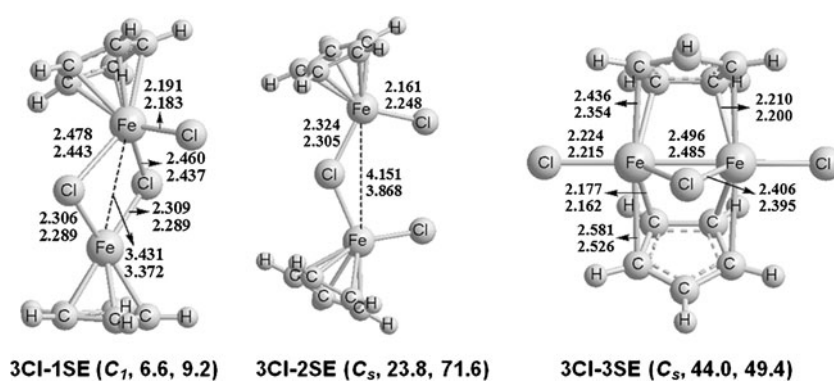
1.86 (MPW1PW91), which is much larger than the ideal value S(S +1) = 0.75. The Fe-Cl distances to the bridging Cl ligand are 2.275 Å (B3LYP) or 2.255 Å (MPW1PW91), and these distances to the terminal Cl ligands are 2.206 Å (B3LYP) or 2.192 Å (MPW1PW91). The Fe-Fe distance in **3Cl-1D** is 2.891 Å (B3LYP) or 2.729 Å (MPW1PW91), which is consistent with the Fe-Fe single bond.

Three sextet $Cp_2Fe_2Cl_3$ structures were found (Fig. 5). Structure **3Cl-1SE** (Fig. 5) is a C_1 structure with two bridging and one terminal Cl ligands. It has all real harmonic frequencies, lying 6.6 kcal mol^{-1} (B3LYP) or 9.2 kcal mol^{-1} (MPW1PW91) above **3Cl-1Q**. The spin contamination in **3Cl-1SE** is very little with $\langle S^2 \rangle$ = 9.04 (B3LYP) or $\langle S^2 \rangle$ = 9.10 (MPW1PW91), which is close to the ideal value S(S + 1) = 8.75. The Fe-Cl distances to the two bridging Cl ligands are in the range of 2.306 to 2.478 Å, and that to the terminal Cl ligand is 2.191 Å (B3LYP) or 2.183 Å (MPW1PW91). The long Fe-Fe distance in **3Cl-1SE** of 3.431 Å Å (B3LYP) or 3.372 Å (MPW1PW91) suggests that there is no direct iron-iron interaction for this structure with two three-electron donor bridging Cl ligands. In addition, the calculated magnetic moment of the binuclear sextet structure **3Cl-1SE** is 5.9μ_B.

The next sextet $Cp_2Fe_2Cl_3$ structure **3Cl-2SE** (Fig. 5) is a C_s structure. Structure **3Cl-2SE** has some spin contamination, i.e., $\langle S^2 \rangle$ = 9.72 by MPW1PW91, which is much larger than that given by B3LYP. It has one bridging and two terminal Cl ligands, lying 23.8 kcal mol^{-1} (B3LYP) or 71.6 kcal mol^{-1} (MPW1PW91) in energy above **3Cl-1Q**. **3Cl-2SE** is predicted to have all real harmonic frequencies by MPW1PW91, but it has an imaginary frequency (75i cm^{-1}) by B3LYP. In **3Cl-2SE**, the Fe-Cl distances to the bridging Cl ligand are 2.324 Å (B3LYP) or 2.305 Å (MPW1PW91), and those to the terminal Cl ligands are 2.161 Å (B3LYP) or 2.248 Å (MPW1PW91). The Fe-Fe distance in **3Cl-2SE** is 4.151 Å (B3LYP) or 3.868 Å (MPW1PW91), clearly indicating the absence of a direct iron-iron bond. Thus, one of the iron atoms in **3Cl-2SE** has a 15-electron configuration but the other iron atom has a 16-electron configuration, consistent with the sextet spin multiplicity. Thus, this leads to five unpaired electrons in **3Cl-2SE**.

Another sextet $Cp_2Fe_2Cl_3$ structure **3Cl-3SE** (Fig. 5) is a C_s perpendicular structure with one bridging and two terminal Cl ligands, lying 44.0 kcal mol^{-1} (B3LYP) or 49.4 kcal mol^{-1} (MPW1PW91) in energy above **3Cl-1Q**. The spin contamination $\langle S^2 \rangle$ for **3Cl-3SE** is 9.59 by B3LYP or 9.74 by MPW1PW91. Structure **3Cl-3SE** has a small imaginary frequency (54i cm^{-1} or 64i cm^{-1}) by B3LYP and MPW1PW91. The Fe-Cl distances to the bridging Cl ligand are 2.406 Å (B3LYP) or 2.395 Å (MPW1PW91), and those to the terminal Cl ligands are 2.224 Å (B3LYP) or 2.215 Å (MPW1PW91). In **3Cl-3SE**, the Fe-Fe distance is 2.496 Å (B3LYP) or 2.485 Å (MPW1PW91).

$Cp_2Fe_2Cl_2$

Three low-lying structures (one triplet and two singlet) were found for $Cp_2Fe_2Cl_2$ with iron in the formal +2 oxidation state (Fig. 6). The global minimum **2Cl-1T** is predicted to be a triplet C_2 doubly bridged structure. The spin contamination for **2Cl-1T** is not serious, i.e., $\langle S^2 \rangle$ = 2.12 (B3LYP) or $\langle S^2 \rangle$ = 2.20 (MPW1PW91). Structure **2Cl-1T** has a small imaginary frequency (8i cm^{-1}) by B3LYP, while this imaginary frequency becomes real when a finer (120, 974) integration grid is used, which indicates that the small imaginary frequency arises from numerical integration error. In **2Cl-1T**, the Fe-Cl distances to the bridging Cl ligand are 2.290 and 2.300 Å (B3LYP) or 2.268 and 2.277 Å (MPW1PW91). The Fe-Fe distance in **2Cl-1T** is 2.410 Å (B3LYP) or 2.378 Å (MPW1PW91), which is consistent with the single bond needed to give both iron atoms the 17-electron configurations, thereby leading to one unpaired electron per Fe atom and the calculated magnetic moment of **2Cl-1T** is 2.8μ_B.

The two singlet $Cp_2Fe_2Cl_2$ structures **2Cl-1S** and **2Cl-2S** are genuine minima with no imaginary vibrational frequencies (Fig. 6). Structure **2Cl-1S** is a C_{2v} structure with two bridging Cl ligands, which has similar geometries to **2Cl-1T**, and lies 8.2 kcal mol^{-1} by B3LYP or 9.6 kcal mol^{-1} by MPW1PW91 above **2Cl-1T**. The Fe-Cl distances to the bridging Cl ligand in **2Cl-1S** are 2.291 Å (B3LYP) or 2.267 Å (MPW1PW91). The Fe-Fe distance in **2Cl-1S** is

Fig. 6 Three optimized structures for $Cp_2Fe_2Cl_2$ indicating the relative energies (ΔE, in kcal mol^{-1}) by the B3LYP and MPW1PW91 methods, respectively

2Cl-1T (C_2, 0.0, 0.0)   2Cl-1S (C_{2v}, 8.2, 9.6)   2Cl-2S (C_2, 36.8, 39.3)
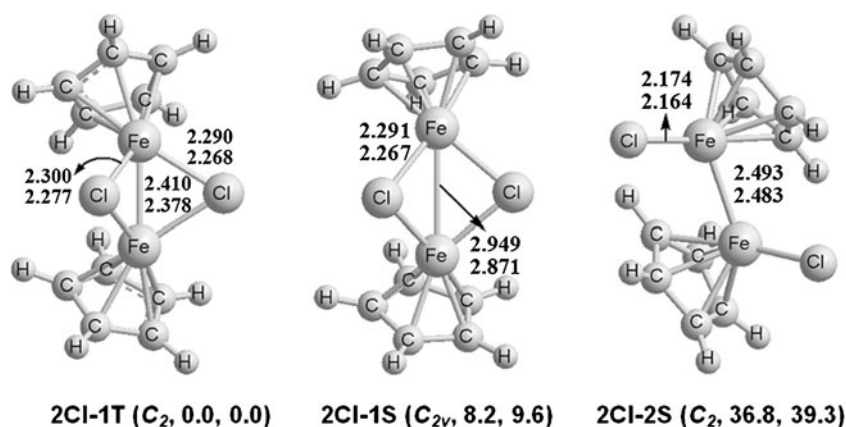
2.949 Å (B3LYP) or 2.871 Å (MPW1PW91), which is about 0.5 Å longer than that in **2Cl-1T**.

The other singlet $Cp_2Fe_2Cl_2$ structure **2Cl-2S** (Fig. 6) is a C_2 trans isomer with two terminal Cl ligands and lies 36.8 kcal mol^{-1} (B3LYP) or 39.3 kcal mol^{-1} (MPW1PW91) above **2Cl-1T**. In **2Cl-2S**, the Fe-Cl distances to the terminal Cl ligands are 2.174 Å (B3LYP) or 2.164 Å (MPW1PW91). The Fe-Fe distance in **2Cl-2S** is 2.493 Å (B3LYP) or 2.483 Å (MPW1PW91), which is found to be shorter than that in the doubly bridged structure **2Cl-1S**.
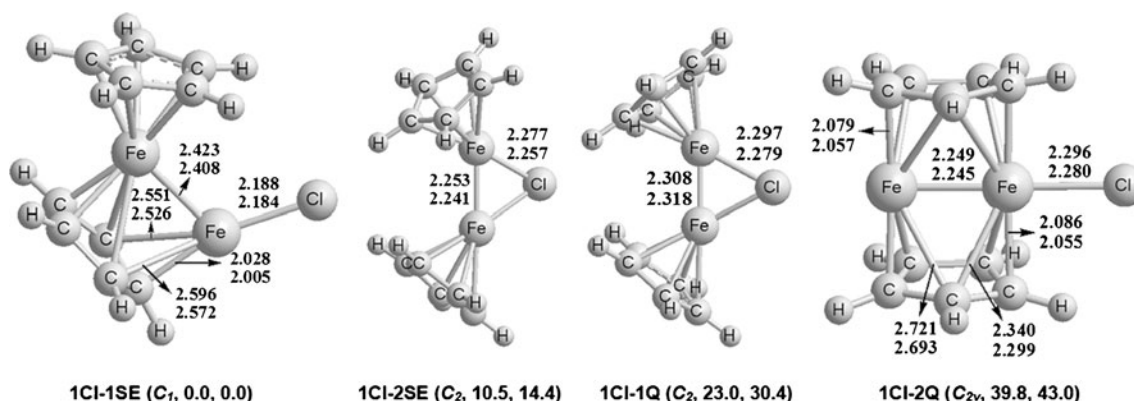
Cp$_2$Fe$_2$Cl

Four energetically low-lying structures were found for Cp_2Fe_2Cl in which the iron atoms have an average formal oxidation state of +1.5 (Fig. 7), including two sextet and two quartet structures. Here, the doublet structures are not shown because of their higher energies. The global minimum for Cp_2Fe_2Cl (**1Cl-1SE**) is a C_1 sextet structure with a terminal Cl ligand, which has all real vibrational frequencies and the calculated magnetic moment is 5.9μ_B. There is relatively small spin contamination, i.e., $\langle S^2 \rangle$ = 8.88 (B3LYP) or 8.91 (MPW1PW91), which is close to the ideal value $S(S+1)$ =

8.75. Structure **1Cl-1SE** is an interesting structure in which one iron atom is bonded to a portion of the two Cp rings and the other iron atom is only bonded to one of the two Cp rings. In **1Cl-1SE**, the Fe-Cl distances to the termial Cl ligand is 2.188 Å (B3LYP) or 2.184 Å (MPW1PW91). The Fe-Fe distance in **1Cl-1SE** is 2.551 Å by B3LYP or 2.526 Å by MPW1PW91, which can be interpreted as a Fe–Fe single bond.

The next energy higher lying structure for Cp_2Fe_2Cl (Fig. 7), namely, the C_2 sextet structure **1Cl-2SE** has a bridging Cl ligand with small spin contamination, i.e., $\langle S^2 \rangle$ = 8.90 (B3LYP) or 8.91 (MPW1PW91). Structure **1Cl-2SE** is predicted to lie 10.5 kcal mol^{-1} (B3LYP) or 14.4 kcal mol^{-1} (MPW1PW91) above the global minimum **1Cl-1SE**. It has all real vibrational frequencies by B3LYP and MPW1PW91. The Fe-Cl distances to the bridging Cl ligand is 2.277 Å (B3LYP) or 2.257 Å (MPW1PW91). The Fe-Fe distance in **1Cl-2SE** is 2.253 Å (B3LYP) or 2.241 Å (MPW1PW91) in **1Cl-2SE**, close to the experimental Fe–Fe triple bond distance (2.177 Å) in the binuclear iron carbonyl derivative [44].

The lowest lying quartet structure of Cp_2Fe_2Cl (Fig. 7), **1Cl-1Q** with C_2 symmetry and a bridging Cl ligand is

1Cl-1SE (C_1, 0.0, 0.0)   1Cl-2SE (C_2, 10.5, 14.4)   1Cl-1Q (C_2, 23.0, 30.4)   1Cl-2Q (C_{2v}, 39.8, 43.0)

Fig. 7 Four optimized structures for Cp_2Fe_2Cl indicating the relative energies (ΔE, in kcal mol^{-1}) by the B3LYP and MPW1PW91 methods, respectively

geometrically similar to **1Cl-2SE**. It has all real vibrational frequencies and lies 23.0 kcal mol^{-1} (B3LYP) or 30.4 kcal mol^{-1} (MPW1PW91) above the global minimum **1Cl-1SE**. Structure **1Cl-1Q** has some spin contamination, $\langle S^2 \rangle$ = 4.31 (B3LYP) or 4.62 (MPW1PW91). In **1Cl-1Q**, the Fe-Cl distances to the bridging Cl ligand is 2.297 Å (B3LYP) or 2.279 Å (MPW1PW91). The Fe-Fe distance in **1Cl-1Q** is 2.308 Å by B3LYP or 2.318 Å by MPW1PW91, which is slightly larger than the experimental Fe–Fe triple bond distance (2.177 Å) in the binuclear iron carbonyl derivative [44].

The second quartet Cp$_2$Fe$_2$Cl stationary point **1Cl-2Q** is a C_{2v} perpendicular structure with one terminal Cl ligand and two bridging Cp rings (Fig. 7), which lies above **1Cl-1SE** by 39.8 kcal mol^{-1} (B3LYP) or 43.0 kcal mol^{-1} (BP86). There is a relatively small degree of spin contamination, i.e., $\langle S^2 \rangle$ = 3.94 (B3LYP) or 4.07 (MPW1PW91). Structure **1Cl-2Q** has a small imaginary vibrational frequencies of 58i cm^{-1} by B3LYP and 80i cm^{-1} by MPW1PW91. In **1Cl-2Q**, each iron atom is bonded to six carbon atoms of the two Cp rings (three carbon atoms from each ring). The Fe-Cl distance to the terminal Cl ligand is 2.296 Å (B3LYP) or 2.280 Å (MPW1PW91). The Fe-Fe distance in **1Cl-2Q** of 2.249 Å (B3LYP) or 2.245 Å (MPW1PW91) is close to the experimental Fe–Fe triple bond distance (2.177 Å) in the binuclear iron carbonyl derivative [44]. The Fe-Fe triple bond gives one iron atom a 16-electron configuration and the other iron atom a 17-electron configuration for a binuclear quartet with three unpaired electrons.

Dissociation, disproportionation and oxidative addition reactions

Table 1 lists the dissociation energies for the reactions Cp$_2$Fe$_2$Cl$_n$ → Cp$_2$Fe$_2$Cl$_{n-1}$ + $\frac{1}{2}$ Cl$_2$ based on the lowest energy structures. The reaction for the loss of one Cl atom from Cp$_2$Fe$_2$Cl$_6$ (**6Cl-1T**) and Cp$_2$Fe$_2$Cl$_5$ (**5Cl-1Q**) are predicted to be exothermic by −12.6 and −3.4 kcal mol^{-1} (B3LYP) or −10.9 and −2.8 kcal mol^{-1} (MPW1PW91), respectively, suggesting that Cp$_2$Fe$_2$Cl$_6$ and Cp$_2$Fe$_2$Cl$_5$ are thermodynamically unstable molecules. This is consistent with the relative instability of high-valent iron species, which are proposed as active intermediates [45]. While the reactions for the loss of one Cl atom from Cp$_2$Fe$_2$Cl$_4$ (**4Cl-1T**), Cp$_2$Fe$_2$Cl$_3$ (**3Cl-1Q**) and Cp$_2$Fe$_2$Cl$_2$ (**2Cl-1T**) are predicted to be

endothermic and the dissociation energies for these reactions are larger than 3.9 kcal mol^{-1}. This indicates that Cp$_2$Fe$_2$Cl$_4$, Cp$_2$Fe$_2$Cl$_3$ and Cp$_2$Fe$_2$Cl$_2$ with iron in formal oxidation states from +1 to +3 appear to be energetically favorable with respect to extrusion of a chlorine atom.

The energies of the disproportionation reactions 2Cp$_2$Fe$_2$Cl$_n$ → Cp$_2$Fe$_2$Cl$_{n+1}$ + Cp$_2$Fe$_2$Cl$_{n-1}$ (Table 2) suggest that Cp$_2$Fe$_2$Cl$_5$, Cp$_2$Fe$_2$Cl$_4$ and Cp$_2$Fe$_2$Cl$_3$ are likely to be thermodynamically stable molecules owing to endothermic disproportionation. However, the analogous disproportionation energy of Cp$_2$Fe$_2$Cl$_2$ into Cp$_2$Fe$_2$Cl$_3$ and Cp$_2$Fe$_2$Cl is predicted to be exothermic by −18.2 kcal mol^{-1} (B3LYP) or −28.4 kcal mol^{-1} (MPW1PW91).

In order to explore the possible synthetic route to these cyclopentadienyl iron chlorides, the oxidative addition reactions of Cp$_2$Fe$_2$Cl$_{n-2}$ + Cl$_2$ → Cp$_2$Fe$_2$Cl$_n$ are also investigated (Table 3). For these reactions of Cp$_2$Fe$_2$Cl (**1Cl-1SE**) and Cp$_2$Fe$_2$Cl$_2$ (**2Cl-2T**), the values of the Gibbs free energy changes are all negative, indicating that Cp$_2$Fe$_2$Cl$_3$ and Cp$_2$Fe$_2$Cl$_4$ may be derived by oxidative addition of Cl$_2$ to Cp$_2$Fe$_2$Cl and Cp$_2$Fe$_2$Cl$_2$, respectively. However, for the oxidative addition reactions of Cp$_2$Fe$_2$Cl$_3$ (**3Cl-1Q**) and Cp$_2$Fe$_2$Cl$_4$ (**4Cl-1T**) to give Cp$_2$Fe$_2$Cl$_5$(**5Cl-1Q**) and Cp$_2$Fe$_2$Cl$_6$ (**6Cl-1T**), the Gibbs free energy changes are larger than 3.7 kcal mol^{-1}. Thus, Cp$_2$Fe$_2$Cl$_3$ and Cp$_2$Fe$_2$Cl$_4$ seem to be more stable than Cp$_2$Fe$_2$Cl$_5$ and Cp$_2$Fe$_2$Cl$_6$ with respect to the oxidative addition reactions, which is consistent with the results of the dissociation reactions (Table 1).

Discussion

The lowest energy structures of Cp$_2$Fe$_2$Cl$_n$ (n=6−1) except for Cp$_2$Fe$_2$Cl have terminal Cp rings and bridging Cl ligands up to a maximum of two bridges. All of these complexes are generally paramagnetic high-spin species with magnetic moments between 2.8μ_B and 5.9μ_B. Therefore, these magnetic complexes can be comparable to the substituted high-spin cyclopentadienyliron complexes [19, 20]. In addition, these high-spin species with odd number of chloride atoms, which are mixed oxidation state derivatives have larger magnetic moments than other species with even number of chloride atoms. Furthermore, the monochloride Cp$_2$Fe$_2$Cl with a terminal Cl ligand has the largest magnetic moment.

Table 1 The dissociation energies (kcal mol^{-1}) including zero-point vibrational energy (ZPVE) corrections for Cp$_2$Fe$_2$Cl$_n$ → Cp$_2$Fe$_2$Cl$_{n-1}$+ $\frac{1}{2}$ Cl$_2$

Reactions	B3LYP	MPW1PW91
Cp$_2$Fe$_2$Cl$_6$ (**6Cl-1T**) → Cp$_2$Fe$_2$Cl$_5$ (**5Cl-1Q**) + $\frac{1}{2}$ Cl$_2$	−12.6	−10.9
Cp$_2$Fe$_2$Cl$_5$ (**5Cl-1Q**) → Cp$_2$Fe$_2$Cl$_4$ (**4Cl-1T**) + $\frac{1}{2}$ Cl$_2$	−3.4	−2.8
Cp$_2$Fe$_2$Cl$_4$ (**4Cl-1T**) → Cp$_2$Fe$_2$Cl$_3$ (**3Cl-1Q**) + $\frac{1}{2}$ Cl$_2$	12.8	3.9
Cp$_2$Fe$_2$Cl$_3$ (**3Cl-1Q**) → Cp$_2$Fe$_2$Cl$_2$ (**2Cl-1T**) + $\frac{1}{2}$ Cl$_2$	59.1	67.3
Cp$_2$Fe$_2$Cl$_2$ (**2Cl-1T**) → Cp$_2$Fe$_2$Cl (**1Cl-1SE**) + $\frac{1}{2}$ Cl$_2$	40.9	39.0

Table 2 The dissociation energies (kcal mol^{-1}) including ZPVE corrections of the disproportionation reactions for the Cp$_2$Fe$_2$Cl$_n$ derivatives

Reactions	B3LYP	MPW1PW91
2Cp$_2$Fe$_2$Cl$_5$ (**5Cl-1Q**) → Cp$_2$Fe$_2$Cl$_6$ (**6Cl-1T**) + Cp$_2$Fe$_2$Cl$_4$ (**4Cl-1T**)	9.2	8.1
2Cp$_2$Fe$_2$Cl$_4$ (**4Cl-1T**) → Cp$_2$Fe$_2$Cl$_5$ (**5Cl-1Q**) + Cp$_2$Fe$_2$Cl$_3$ (**3Cl-1Q**)	16.2	6.6
2Cp$_2$Fe$_2$Cl$_3$ (**3Cl-1Q**) → Cp$_2$Fe$_2$Cl$_4$ (**4Cl-1T**) + Cp$_2$Fe$_2$Cl$_2$ (**2Cl-1T**)	46.3	63.5
2Cp$_2$Fe$_2$Cl$_2$ (**2Cl-1T**)→Cp$_2$Fe$_2$Cl$_3$ (**3Cl-1Q**) + Cp$_2$Fe$_2$Cl (**1Cl-1SE**)	−18.2	−28.4

The global minimum structure of Cp$_2$Fe$_2$Cl$_6$ (Fig. 1) in which the iron atoms are in the +4 formal oxidation state is the triplet singly bridged structure **6Cl-1T** with two unpaired electrons and a long non-bonding Fe-Fe distance of ~4.0 Å. In **6Cl-1T**, the bridging chlorine atom (considered as a neutral ligand) is formally a two-electron donor to one iron atom and a one-electron donor to the other iron atom, giving each iron atom the 17-electron configuration. Thus, the calculated magnetic moment of **6Cl-1T** is 2.8μ_B.

The lowest energy Cp$_2$Fe$_2$Cl$_5$ structure **5Cl-1Q** (Fig. 2) with the iron atom in an average +3.5 oxidation state is a *trans* quartet structure. **5Cl-1Q** has one bridging and four terminal chlorine atoms with three unpaired electrons, and the calculated magnetic moment of **5Cl-1Q** is 3.9μ_B. The predicted Fe-Fe distance in **5Cl-1Q** is ~4.0 Å, indicating the absence of a direct iron-iron bond and giving one iron atom in **5Cl-1Q** a 16-electron configuration but the other iron atom a 17-electron configuration.

The lowest lying Cp$_2$Fe$_2$Cl$_4$ structure **4Cl-1T** (Fig. 3) with iron in the formal +3 oxidation state is a *trans* dibridged triplet structure, which has two unpaired electrons and the calculated magnetic moment is 2.8μ_B. The distance between the two iron atoms in **4Cl-1T** is very long, namely, ~3.3 Å, clearly indicating the absence of a direct bond. This allows each iron atom in **4Cl-1T** to achieve the 17-electron configuration.

The trichloride Cp$_2$Fe$_2$Cl$_3$ (Figs. 4 and 5) with one Fe(II) atom and one Fe(III) atom is formally a mixed valence compound with an average iron oxidation state of +2.5. The global minimum Cp$_2$Fe$_2$Cl$_3$ structure is the quartet **3Cl-1Q** (Fig. 4) with one bridging Cl ligand and two terminal Cl ligands. **3Cl-1Q** has three unpaired electrons and the calculated magnetic moment is 3.9μ_B. The Fe-Fe distance in **3Cl-1Q** is ~3.0 Å indicating the lack of a direct iron-iron bond.

The lowest energy structure of the dichloride Cp$_2$Fe$_2$Cl$_2$ **2Cl-1T** is a triplet C_2 structure with iron in the formal +2 oxidation state as well as two bridging Cl ligands and two terminal Cp rings (Fig. 6). **2Cl-1T** has two unpaired electrons and the calculated magnetic moment of **2Cl-1T** is 2.8μ_B. The Fe-Fe distance in **2Cl-1T** is predicted to be ~2.4 Å in accord with the single bond required to give each iron atom a 17-electron configuration consistent with the triplet electronic state.

The monochloride Cp$_2$Fe$_2$Cl with one Fe(II) atom and one Fe(I) atom is formally a mixed oxidation state derivative with an average iron formal oxidation state of +1.5. The global minimum **1Cl-1SE** (Fig. 7) is a sextet structure with one terminal Cl ligand. **1Cl-1SE** has five unpaired electrons and possesses the largest magnetic moment (5.9μ_B) among these cyclopentadienyliron chlorides. In **1Cl-1SE**, one iron atom is bonded to a portion of the two Cp rings but the second iron atom bonded to a portion of one Cp ring and the Cl ligand. Structure **1Cl-1SE** has a Fe-Fe distance of about 2.5 Å.

A study of the dissociation reaction Cp$_2$Fe$_2$Cl$_n$ → Cp$_2$Fe$_2$Cl$_{n-1}$ + ½ Cl$_2$ suggests that the Cp$_2$Fe$_2$Cl$_6$ and Cp$_2$Fe$_2$Cl$_5$ derivatives with the iron atoms in an average + 4 and +3.5 oxidation states, respectively, are likely to be thermodynamically disfavored molecules. This also proved that the high-valent iron species have relative instability in most coordination environments [45]. Whereas, the lowest energy structures Cp$_2$Fe$_2$Cl$_3$ and Cp$_2$Fe$_2$Cl$_4$ can be formally derived from the lowest energy Cp$_2$Fe$_2$Cl and Cp$_2$Fe$_2$Cl$_2$ structures by oxidative addition of Cl$_2$, respectively. The Cp$_2$Fe$_2$Cl$_5$, Cp$_2$Fe$_2$Cl$_4$ and Cp$_2$Fe$_2$Cl$_3$ structures are predicted to be thermodynamically stable molecules with respect to endothermic disproportionation reactions.

Conclusions

The lowest energy structures of the cyclopentadienyliron derivatives Cp$_2$Fe$_2$Cl$_n$ ($n=6-1$) are all predicted to be high-spin species, which are potential paramagnetic materials and the calculated magnetic moments are from 2.8μ_B to 5.9μ_B. Compared to the complexes with even number of

Table 3 The Gibbs free energy changes (kcal mol^{-1}) including ZPVE corrections and thermal corrections for Cp$_2$Fe$_2$Cl$_{n-2}$ + Cl$_2$ → Cp$_2$Fe$_2$Cl$_n$

Reactions	B3LYP	MPW1PW91
Cp$_2$Fe$_2$Cl (**1Cl-1SE**) + Cl$_2$ → Cp$_2$Fe$_2$Cl$_3$ (**3Cl-1Q**)	−90.1	−96.0
Cp$_2$Fe$_2$Cl$_2$ (**2Cl-1T**) + Cl$_2$ → Cp$_2$Fe$_2$Cl$_4$ (**4Cl-1T**)	−63.9	−61.1
Cp$_2$Fe$_2$Cl$_3$ (**3Cl-1Q**) + Cl$_2$ → Cp$_2$Fe$_2$Cl$_5$(**5Cl-1Q**)	3.7	11.3
Cp$_2$Fe$_2$Cl$_4$ (**4Cl-1T**) + Cl$_2$ → Cp$_2$Fe$_2$Cl$_6$ (**6Cl-1T**)	26.6	24.7

chloride atoms, species with odd number of chloride atoms as well as the iron atoms in the mix oxidation states have larger magnetic moments, and Cp_2Fe_2Cl possesses the largest magnetic moment. All of the high-spin species have terminal Cp rings and bridging chlorine atom up to a maximum of two bridges except for Cp_2Fe_2Cl. The $Cp_2Fe_2Cl_5$, $Cp_2Fe_2Cl_4$ and $Cp_2Fe_2Cl_3$ structures appear to be stable according to the disproportionation reactions. The lowest energy $Cp_2Fe_2Cl_n$ ($n=3, 4$) structures can be formally derived from the lowest energy $Cp_2Fe_2Cl_n$ ($n=1, 2$) structures by oxidative addition of Cl_2, respectively. However, with respect to the dissociation reactions $Cp_2Fe_2Cl_n \rightarrow Cp_2Fe_2Cl_{n-1} + \frac{1}{2} Cl_2$, $Cp_2Fe_2Cl_6$ and $Cp_2Fe_2Cl_5$ with iron in the formal $+4$ and $+3.5$ oxidation states are likely to be thermodynamically disfavored molecules.

References

1. Kealy TJ, Pauson PL (1951) Nature 168:1039
2. Rogers RD, Atwood JL, Foust D, Rauch MD (1981) J Cryst Mol Struct 11:183
3. Flower KR, Hitchcock PB (1996) J Organomet Chem 507:275
4. Bunder W, Weiss E (1975) J Organomet Chem 92:65
5. Seiler P, Dunitz JD (1980) Acta Crystallogr B 36:2255
6. Albright TA, Burdett JK, Wangbo M-H (1985) Orbital interactions in chemistry.John Wiley, New York
7. Parshall GW (1987) Organometallics 6:687
8. Green MLH, Qin J, O'Hare DJ (1988) Organomet Chem 358:375
9. Miller JS, Epstein AJ, Reiff WM (1988) Chem Rev 88:201
10. Baker WA, Bobonich HM (1964) Inorg Chem 3:1184
11. Watanabe M, Sato M, Nagasawa A, Motoyama I, Takayama T (1998) Bull Chem Soc Jpn 71:2127
12. Watanabe M, Iwamoto T, Nakashima S, Sakai H, Motoyama I, Sano H (1993) J Organomet Chem 448:167
13. Sitzmann H (2001) Coord Chem Rev 214:287
14. Blaha JP, Bursten BE, Dewan JC, Frankel RB, Randolph CL, Wilson BA, Wrighton MS (1985) J Am Chem Soc 107:4561
15. Sharp PR, Bard AJ (1983) Inorg Chem 22:2689
16. Hermes AR, Girolam GS (1987) Organometallics 6:763
17. Hamon P, Toupet L, Hamon J-R, Lapinte C (1994) J Chem Soc Chem Commun 931
18. Hamon P, Toupet L, Hamon J-R, Lapinte C (1996) Organometallics 15:10
19. Sitzmann H, Dezember T, Kaim W, Baumann D-CF, Stalke D, Kärcher D-CJ, Dormann E, Winter H, Wachter D-PC, Kelemen D-PM (1996) Angew Chem Int Ed Engl 35:2872
20. Walter MD, White PS (2011) New J Chem 35:1842
21. Ehlers AW, Frenking G (1994) J Am Chem Soc 116:1514
22. Delley B, Wrinn M, Lüthi HP (1994) J Chem Phys 100:5785
23. Li J, Schreckenbach G, Ziegler T (1995) J Am Chem Soc 117:486
24. Jonas V, Thiel W (1995) J Chem Phys 102:8474
25. Barckholtz TA, Bursten BE (1998) J Am Chem Soc 120:1926
26. Niu S, Hall MB (2000) Chem Rev 100:353
27. Macchi P, Sironi A (2003) Coord Chem Rev 238:383
28. Carreon JL, Harvey JN (2006) Phys Chem Chem Phys 8:93
29. Bühl M, Kabrede H (2006) J Chem Theory Comput 2:1282
30. Becke AD (1993) J Chem Phys 98:5648
31. Lee C, Yang W, Parr RG (1988) Phys Rev B 37:785
32. Adamo C, Barone V (1998) J Chem Phys 108:664
33. Becke AD (1988) Phys Rev A 38:3098
34. Perdew JP (1986) Phys Rev B 33:8822
35. Feng X, Gu J, Xie Y, King RB, Schaefer HF III (2007) J Chem Theory Comput 3:1580
36. Zhao S, Li Z-H, Wang W-N, Liu Z-P, Fan K-N (2006) J Chem Phys 124:184102
37. Dunning TH (1970) J Chem Phys 53:2823
38. Huzinaga S (1965) J Chem Phys 42:1293
39. Wachters AJH (1970) J Chem Phys 52:1033
40. Hood DM, Pitzer RM, Schaefer HF (1979) J Chem Phys 71:705
41. Frisch MJ, Trucks GW, Schlegel HB et al (2003) Gaussian 03, Revision B.03. Gaussian Inc, Pittsburgh (see Supporting Information for details)
42. Papas BN, Schaefer HF (2006) J Mol Struct (THEOCHEM) 768:175
43. Mitschler A, Rees B, Lehmann MS (1978) J Am Chem Soc 100:3390
44. Murahashi S-I, Mizoguchi T, Hosokawa T, Moritani I, Kai Y, Kohara M, Yasuoka N, Kasai N (1974) J Chem Soc Chem Commun 14:563
45. Scepaniak JJ, Vogel CS, Khusniyarov MM, Heinemann FW, Meyer K, Smith JM (2011) Science 331:1049